

# Network Aware Compute and Memory Allocation in Optically Composable Data Centres with Deep Reinforcement Learning and Graph Neural Networks

ZACHARAYA SHABKA<sup>1,\*</sup> AND GEORGIOS ZERVAS<sup>1</sup>

<sup>1</sup>Optical Networks Group, Department of Electronic and Electrical Engineering, University College London, Roberts Building, Torrington Place, London, WC1E 7JE, United Kingdom

\*Corresponding author: zacharaya.shabka.18@ucl.ac.uk

Compiled November 7, 2022

Resource-disaggregated data centre architectures promise a means of pooling resources remotely within data centres, allowing for both more flexibility and resource efficiency underlying the increasingly important infrastructure-as-a-service business. This can be accomplished by means of using an optically circuit switched backbone in the data centre network (DCN); providing the required bandwidth and latency guarantees to ensure reliable performance when applications are run across non-local resource pools. However, resource allocation in this scenario requires both server-level *and* network-level resource to be co-allocated to requests. The online nature and underlying combinatorial complexity of this problem, alongside the typical scale of DCN topologies, makes exact solutions impossible and heuristic based solutions sub-optimal or non-intuitive to design. We demonstrate that *deep reinforcement learning*, where the policy is modelled by a *graph neural network* can be used to learn effective *network-aware* and *topologically-scalable* allocation policies end-to-end. Compared to state-of-the-art heuristics for network-aware resource allocation, the method achieves up to 20% higher acceptance ratio; can achieve the same acceptance ratio as the best performing heuristic with  $3\times$  less networking resources available and can maintain all-around performance when directly applied (with no further training) to DCN topologies with  $10^2\times$  more servers than the topologies seen during training. © 2022 Optica Publishing Group

<http://dx.doi.org/10.1364/ao.XX.XXXXXX>

## 1. INTRODUCTION

Contemporary data centre network (DCN) architectures are based on (opto-)electronically packet-switched (EPS) networks. In a typical Cloud computing model, large tasks requiring more than one server's worth of resources for a long period of time can be distributed across numerous servers, which are all connected via this underlying EPS infrastructure. These allocations can not be done across single inter-server resource pools, instead requiring the task to be split into smaller tasks where each will be allocated resources from and run on a single server [1].

Firstly, bandwidth is limited by the bandwidth per-port of the opto-electronic switches which is fixed per-model. Popular EPS switches typically support a per-port bandwidth at the order of  $\mathcal{O}(1\text{Gb/s}) - \mathcal{O}(10\text{Gb/s})$ , whereas intra-server communications (e.g. L1-cache access by the CPU) often operate at the order of  $\mathcal{O}(Tb/s)$ . For resources to access each other remotely, a large number of ports would be required for just a single pair of devices and networking component costs would increase. Such devices also have fixed bandwidth, meaning higher bandwidth

servers require network infrastructure replacement or must be run sub-optimally.

Secondly, the unpredictable queuing patterns in packet-switched networks lead to non-deterministic latency. Compute mediums (i.e. CPU, GPU, RAM) co-located on the same server exchange information at very high rates. For example, L1 cache latency on high-end desktop CPUs exist in the  $\mathcal{O}(ns) - \mathcal{O}(10ns)$  range. Application performance is strongly dependent on compute-memory latency [2]. EPS networks are incapable of consistently supporting standard application performance given typical forwarding latency is non-deterministic and in the range  $\mathcal{O}(10\mu s) - \mathcal{O}(100\mu s)$ . These features of EPS DCNs lead to two primary resource allocation limitations when allocating large quantities of resources to single tasks for some extended period of time:

**Resource fragmentation** means that resources can become 'stranded' on a particular server, neither in use by any applications running on that server, nor accessible by those running on any others; while sufficient resources for some task may exist collectively across several servers in a DC, they cannot be

co-assigned to said task and are effectively wasted.

**Inflexible resource-pooling** relates to the strict upper limit in resource pool size. In modern EPS-based DCs, this is limited to the amount of resources that can be hosted on a single server, since inter-server resources cannot communicate with the means required to not disrupt application performance. Using pools larger than this requires further consideration about how applications can be effectively divided into sub-applications and distributed, often incurring some runtime-overhead.

Resource disaggregated DCs are a proposed DC architecture supporting a network architecture that provides sufficient bandwidth and latency guarantees for resource pools to be defined across servers on which long-lived resource-hungry applications can be run with local-like performance. This would reduce fragmentation, as well as increase pooling flexibility. Such architectures can in fact be built using off-the-shelf commodity hardware such as commercially available optical-circuit switches [3–6]. However, since both server- and network- resources need to be explicitly provisioned in order to allocate both compute and connectivity, allocation is more complex as decisions need to be made across the product of both of these domains, rather than only server resources as in conventional resource management frameworks [7–10]. This paper will refer to this requirement as *network aware resource allocation*.

This paper shows that deep reinforcement learning (DRL) with graph neural network (GNN) based policies can learn very effective network aware allocation policies end-to-end. Acceptance rate, CPU utilisation and memory utilisation are improved by up to 19%, 24% and 22% respectively compared to state-of-the-art heuristics. Furthermore the DRL-based method achieves approximately the same performance as the best heuristic achieves when it is using  $3\times$  more network resources. While the method is trained on small DCN topologies with  $\mathcal{O}(10^1)$  servers, the GNN-based policy architecture is topology-size agnostic. Because of this it can be directly applied to topologies with  $10^2\times$  more servers than seen during training and maintain its allocation performance without further training required. Following this, a discussion on interpreting the learnt policy is presented, indicating that the method is flexible under changing network resource profiles and generally more adaptable than the heuristics.

## 2. PREVIOUS WORK

Deep learning has been leveraged to tackle numerous online combinatorial optimisation (CO) problems. Pointer networks were introduced as a supervised means of doing so in [11], where this premise was integrated into a DRL framework in [12]. Similarly, a similar methodology was applied to a simple multi-resource cluster allocation problem in [13]. Following this, [14] proposed that when solving combinatorial optimisation problems defined on graphs (e.g. travelling salesperson, max-cut and so on) it should be useful to account for some topological information in the optimisation process. A DRL-based framework for solving CO problems where policies were modelled with GNNs was proposed where GNNs are used to generate node-embeddings which can be used in some selection process to more accurately construct a solution to the underlying problem. Further iterations of this framework have shown it able to scale to graphs with the order of  $\mathcal{O}(10^7) - \mathcal{O}(10^9)$  nodes with similar orders of edges [15–17], perform competitively against exact solvers [18]. This architecture has been used to effectively solve a number of network and computer-system based opti-

misation problems, such as distributed machine learning [19], cluster management with dependency-structured tasks [20], optical routing [21] and virtual network embedding [22, 23].

Network aware algorithms for optically composable disaggregated data centres are described in [4, 5, 24]. These works augment a breadth-first-search procedure to recursively discover sub-networks that can support the required compute, memory, storage, bandwidth and/or latency by some given request. They show advantages over traditional packing algorithms such as best fit, but suffer from poor scalability since they are exhaustive in the worst case. A bandwidth-aware multi-resource cluster allocation (and scheduling) method is described in [25], where servers are ranked based on server-local compute and network resources. However, this has limited exposure to the network as it does not consider network resources multiple hops away from the server. Previous work has shown that DRL with GNN-based policies can be used to learn network aware resource allocation algorithms in composable data centres which are both high performing and scalable [26]. This work continues the examination of these architectures in a similar experimental setting, but analyse more extensively the nature of the policy that is learnt. Specifically, our analysis is extended to the network usage, fairness and general nature of the decision making by the DRL agent. In this way we seek to understand more intuitively what the agent is doing, as opposed to a more simple observation of improved long-term allocation outcomes. We discuss new results about how each tier's network resources are used by the agent (and comparative methods) across the test topologies, as well as analyse the relationship between request size and how the agent's allocations are distributed within racks, between racks and between clusters.

## 3. BACKGROUND

### A. Deep Reinforcement Learning

Reinforcement learning relates to the study of how to find optimal behavioural policies in dynamic environments. When rewards are returned to an actor based on the effect that their action had on the environments state, the goal of a reinforcement learning problem is to find a policy that maximises the reward achieved by an agent over time. A environment is formally described by a *Markov Decision Process* (MDP) defined as a tuple  $\langle S, A, R_a, T_a \rangle$  where:  $S$  is the set of all possible states that the MDP can be in,  $A$  is the set of all possible actions that some actor can take in this environment,  $R_a$  is a function describing the reward yielded when an agent is in state  $s$ , takes action  $a$  and ends up in state  $s'$ , and  $T_a$  is a function describing the probability of an agent being in state  $s$ , taking action  $a$  and ending up in state  $s'$ . Episodes can also be episodic meaning that there is some state after which the environment no longer changes state (e.g. a check-mate position in a chess game environment). A policy is described as some function,  $\pi(s) \rightarrow a$  which maps states to actions, and an optimal policy is one which - if followed - will yield the highest possible reward in that MDP. A very extensive description of RL from first principles can be found in [27].

Deep reinforcement learning is an extension of this generic problem description, to the case where  $\pi(s)$  modelled using deep neural networks. In contrast to older methods (such as table-based policies) has allowed for much greater complexity to be learnt by the policy, as well as greater generalisability when a policy is exposed to a previously unseen state. Such developments have seen DRL exceed human performance in considerably complex tasks like the board game of Go and the

video game Starcraft [28, 29].

### A.1. Graph Neural Networks

Graph neural networks extend standard neural network (NN) architectures to graph-structured data, where data points are nodes and any relationships (e.g. a friendship between two people in a social network) are represented by edges. GNNs attempt to account for topological information as well as the raw data during learning tasks. This is accomplished by means of a *message passing procedure* where node (and possible edge) information is propagated through the network via nearest-neighbour exchanges and aggregated at nodes. These aggregations are then used as a new representation of each node, which can be processed by some NN structure. This procedure can be repeated (for all nodes simultaneously) in order to propagate information further through the network, and as such the final output of the GNN for each node is one which accounts for information about itself, it's neighbours and local network region. This procedure can be represented by the equation:

$$h_v = g(v, \sum_{v' \in N(v)} f(v', e_{v,v'})) \quad (1)$$

where  $g$  and  $f$  are (learnable) functions,  $v$  is the information at node  $v$ ,  $e_{v,v'}$  is the information at the edge connecting nodes  $v$  and  $v'$ ,  $N(v)$  is the set of all one-hop neighbours of node  $v$  and  $h_v$  is the new representation of node  $v$  after a single message passing procedure has been applied. In the case of a GNN,  $g$  and  $f$  will generally be implemented with a neural network. GNN architectures have shown to yield richer node embeddings than classical node-embedding methods (e.g. PageRank) and can outperform these methods in statistical tasks such as graph clustering or node classification [30–32].

### A.2. Combinatorial Optimisation

Combinatorial optimisation (CO) problems describe scenarios with a finite set of items, where some optimal sub and/or ordered set of items (often termed the *solution*) must be determined. Typically there will be some validity criteria for a solution such that some solutions do not have a value (e.g. a solution that does not traverse every node once and only once in a travelling salesperson problem is not valid). Formally, a CO problem can be described by a set of instances,  $I$  (an instance could be a particular set of bins in a bin packing problem); for some instance  $x \in I$ ,  $f(x)$  is the set of valid solutions and  $m(x, y)$  (termed the objective function) maps some valid solution  $y \in f(x)$  to some number; the goal of a CO problem is to find, for some  $x \in I$ , a solution  $y' \in f(x)$  such that  $m(x, y')$  is either minimised or maximised (depending on the problem).

There are no formal constraints on how solutions can be constructed. They can be either determined entirely and then evaluated (as in some exact solvers) or they can be iteratively constructed by adding items one at a time and continuously evaluating whether the current solution is valid, and if so what is its objective value. For graph-based CO problems (e.g. routing, min-cut etc), solutions can often be built by iteratively adding nodes from the graph to the solution set (as will be implemented in this paper).

## 4. PROBLEM

In this paper we present the problem as online network aware resource allocation in disaggregated data centre systems as a

MDP and show that GNN-based DRL can be leveraged effectively to solve this problem. This section will describe how the MDP is defined including the request/resource allocation dynamics of the underlying DCN, the learning architecture used to model the policy, the experiments carried out and the baselines used for comparison.

### A. Defining the Markov Decision Process

**Environment:** The environment consists of a set of servers, a network interconnecting these servers via some network switches and requests which arrive one by one. This DCN environment is also visualised in A.

The DC/DCN consists of the servers + network and is represented by a graph,  $G(V, E)$ . Each server (represented by the set of nodes  $V \in G$ ) has an associated resource vector. Specifically, in this problem the CPU and memory resources are accounted for so that  $[v_{cpu}, v_{mem}] \forall v \in V$ , where  $v_{cpu}$  &  $v_{mem}$  represent the available CPU and memory resources of server  $v$  at any given moment.

Similarly, each switch has a particular number of input and output ports. This is represented by proxy using edge features, such that each edge has a number of distinct channels, also denoted by a resource vector  $[e_{ch}] \forall e \in E$  where  $e_{ch}$  is the number of available channels in that link. This represents a scenario where a certain number of ports on a switch are reserved for a particular server who's direct link to that switch has a certain number of channels.

**Table 1.** Oversubscription and number of channels per link for each topology. 'Bottom-top oversubscription' refers to the oversubscription from the servers to the top tier of switches (tier-3). 'Oversub' refers to the oversubscription at the interface between that tier and the tier below it (hence Tier-1 does not have an 'oversub' value. In this work we used topologies of this structure with  $n \in \{8, 16, 32\}$ ).

Oversubscription, channels-per-link for network tiers			
	Bottom-top Oversubscription		
	1:16	1:8	1:4
	Ovsub, Chan	Ovsub, Chan	Ovsub, Chan
Tier-1	-, $n$	-, $n$	-, $n$
Tier-2	1:4, $2n$	1:2, $4n$	1:2, $4n$
Tier-3	1:4, $\frac{1}{2}n$	1:4, $n$	1:2, $2n$

Requests arrive at the RDDC one at a time and are not seen in advance, where  $R = [r_{cpu}, r_{mem}, r_t]$  represents the CPU, memory and holding time requirements for that request. A valid solution consists of a set of nodes,  $V'$ , must be found such that  $\sum v_x \in V' \geq r_x, x \in \{cpu, mem\}$  and a set of  $\frac{|V'|(|V'|-1)}{2}$  distinct paths can be found to guarantee all-to-all connectivity between all  $v \in V'$ . A good solution to this problem is one which maximises successful allocations over time.

**Episode:** An episode is defined as receiving  $N$  requests. For each request the agent will iteratively choose servers until either it has successfully allocated a request or its solution is invalid. When a new request arrives, if there is enough raw resources available in the DCN to theoretically allocate it, the agent is



prompted to attempt to do so. If a valid solution is generated (there are not enough network resources available to connect all servers in the allocation) then this request is dropped and a new request is fetched. We do not model queuing as this involves another algorithmic domain (to balance new and queued request with priority structures etc) and in this work we wish to focus on the network-awareness/congestion dynamics of the underlying system. Moreover, queuing/prioritising can be handled in parallel to resource allocation decisions so can be considered separately.

**State:** given an awaiting request  $R = \{r_{cpu}, r_{mem}, r_t\}$  (CPU, memory and holding-time requirements respectively) the MDP's state is

$$s = \{G(V_{norm}, E), r_t, U_{cpu}, U_{mem}\} \quad (2)$$

where,  $V_{norm} = \{\frac{v_x}{r_x} \forall v_x \in V\}$ ,  $x \in \{cpu, mem\}$  and  $U_x$  is the RDDC-global utilisation of resource  $x \in \{cpu, mem\}$ . This combines both node-, edge- and graph- level resource information within the state representation.

Feature normalisation is important in machine learning problems to ensure that certain features with larger absolute values/variation do not disproportionately influence policy updates during training. Furthermore, normalised state representation ensures that policies should be robust under testing on similar environments differing only by absolute scales (e.g. a DCN with 4 CPU units-per-server vs one with 16 units-per-server, or a scenario where requests are between 1-8 servers vs one where they are between 8-16). As such, each server's resource values are normalised with respect to the current requested amount of that resource. Similarly, link-resources are normalised with respect to the maximum initial amount on any link in the DCN. This ensures that the policy is exposed to the DCN in a way that is feature-scale agnostic, as well as agnostic to the relative scale of request quantities and server-resource quantities.

**Action:** A server  $v \in V$  is added to  $V'$ . If constraint 2 defined previously cannot be satisfied (when  $k=3$  shortest paths are tried per node-pair) the allocation fails. If constraint 2 is satisfied, then  $\max(v_x, r_x)$  - the maximum that can be provisioned from this server up to the limit of how much is needed and how much is present at that server - from  $v (x \in \{cpu, mem\})$  and one channel-per-link per-path per-node-pair are allocated. If constraint 1 & 2 are satisfied the allocation is successful. Per request, actions are taken until an action succeeds or fails an allocation, at which point a new request is fetched (until termination).

**Reward:** An agent will receive  $\alpha$  if the action is successful,  $\beta$  if the action is unsuccessful,  $\gamma$  otherwise where 10, -10 and 0 were used for  $\alpha$ ,  $\beta$  and  $\gamma$  respectively. Rewarding 0 for intermediate decisions (i.e. when servers have been chosen but the request has neither failed nor been accepted) ensures that the reward is agnostic to the allocation choices. More generally, the reward is kept very simple and only based on allocation success or lack thereof for each request. This is done to minimise the influence on the kind of policies that the agent might learn. For example, if small negative intermediate rewards were given to incentivise allocating across as few servers as possible, this would likely not allow the agent to explore policies where allocating across lots of servers is sometimes preferable. More generally, one of the main motivations behind this work is that hand-designing heuristics is non-intuitive for complex systems or problems. As such, by simplifying the reward structure as much as possible and relating it only to a generic high level goal (allocate as many requests as possible over time), the designers are not meaningfully influencing the specific policy that the agent learns and

allow it a more arbitrary exploration of possible solutions during training.

## B. Defining the deep reinforcement learning model

The learning model consists of a GNN (based on the GraphSAGE architecture [31]) and 2 deep neural networks (DNN) which we refer to as  $DNN_1$  and  $DNN_2$ . The GNN acts on  $G(V_{norm}, E)$  to generate embeddings of each node in the topology.  $DNN_1$  outputs a high dimensional representation of  $[r_t, U_{cpu}, U_{mem}]$ .  $DNN_2$  then calculates logits for each node in the RDDC graph based on an input of the concatenation of the GNNs embedding of that node, the output of  $DNN_1$  and the element-wise mean of the embeddings of the nodes that have already been allocated to that request (or a zero-vector if the request has just been received and nothing has been allocated yet). These logits are passed through a softmax function to specify the probability of choosing each node. This model is used to approximate a policy, trained using the proximal policy optimisation (PPO) RL algorithm, and is implemented using RLlib and Deep Graph Library [33, 34].

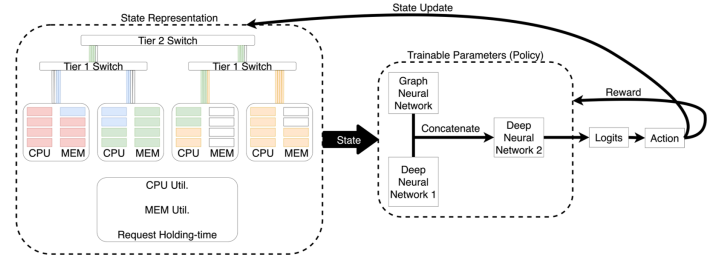


**Fig. 1.** High-level diagram of the RDDC + model + RL feedback loop implemented in this work.

The GNN used a distinct mean-based aggregator for each layer, where messages exchanged during the message passing process are aggregated like:

$$v = \frac{1}{|N(v)| + 1} \sum_{x \in M_v} W_i(x) \quad (3)$$

where  $v$  is a node (embedding) in the RDDC graph  $G(V, E)$ ,  $N(v)$  is the set of the one-hop neighbours of  $v$ ,  $M_v$  is the set of messages received by  $v$  from its neighbours and  $W_i$  is a neural network associated with the  $i^{th}$  layer of the GNN.

The GNN outputs embeddings of each node in 16 dimensions, and 3 layers were used so that information from the top of the network can be accounted for in the embeddings of the servers.

We compare our model against 3 baselines (Tetris, NALB, NULB) from previous work as well as a random allocation policy [5, 24, 25].

## 5. EXPERIMENTAL SETUP

### A. Training and Testing

Servers initially have 16 units of both CPU and memory resources. We use 12 different 3-tier as detailed in table 1. This is visualised in Fig. 7 in Appendix A. The values for channels-per-link in tier-1 (i.e. max number of other servers that a server connect to) is  $\{8, 16, 32\}$  and the set of bottom-to-top oversubscription ratios is  $\{1:4, 1:8, 1:16\}$ , where tier-2 and tier-3 channel values are set to ensure these ratios given the number of channels in a tier-1 link. Higher oversubscription (lower ratio) imposes a

stronger mandate for rack-locality on allocations due to limited upper-tier network resources. Less tier-1 channels per server limits how many servers an allocation can be spread across, since all server within an allocation must be interconnected. Topologies used for training and testing have 64 nodes (2 clusters  $\times$  2 racks  $\times$  16 servers). Trained models were also tested on graphs the order of  $10^2$  times larger with respect to number of nodes (8 clusters  $\times$  8 racks  $\times$  16 servers) with episodes of 2048 requests. Requests are uniformly sampled with a maximum request size of 8 full-servers worth of resources in each domain (128 units), and their holding times are sampled such that the average offered load on the RDDC system is 95% of all CPU and memory resources. Separate agents are trained for each topology, and tested against each baseline on that same topology.

Training episodes are terminated after 32 requests have been received (successfully or otherwise) by the agent, and testing episodes on the smaller topology are terminated after 128 requests have been received. Shorter training episodes are generally more desirable since it is easier for the agent to receive meaningful reward signals [35, 36] (provided that the shortness of the episode is not so much so that some important dynamic/feature of the underlying environment is not experienced by the learning agent). On the other hand, in the scenario explored here, any trained agent deployed in some real DC scenario would be operating in an effectively infinitely long episode (i.e. it will continue to allocate resources to requests as long as the DC environment it manages is in use). As such it is important to ensure that the policy learnt is not limited in performance to just the short episodes seen during training. The training episode length is chosen long enough for all tested baselines to be at a ‘stable’ performance level for the majority of the episode. For a short episode, much of the time is spent allocating the first requests when most of the resources are still available (sometimes referred to as ‘warm up’). While warm up strategy is important (bad decisions early on can cascade into long term inefficiencies), the performance statistics at the end of this phase are not indicative of long term performance where utilisation is consistently high as more requests are received. Testing episodes are therefore longer than training ones to emphasise performance on the long-term dynamics of the system (more akin to real DC system operation). Testing episodes are seeded in the same way for each baseline, so all methods are exposed to the same set of requests (per test) received in the same order. Each test is run 5 times and results presented (where a single value per topology is shown) are the average of these 5 runs.

As noted, tests are also implemented on scaled up ( $\mathcal{O}(10^3)$  nodes) versions of each respective topology. Much longer episodes are required here since warm up takes much longer (since there is  $\mathcal{O}(10^2) \times$  more resources in the DCN). Additionally, in order to maintain a high offered load the holding times are increased appropriate so that resource requirements build up in the system and allocation becomes harder as more requests arrive. More crucially, this test is done to explore the suitability of this method in a real DCN allocation scenario. Server clusters in large enterprise computer networks are of the order of  $\mathcal{O}(10^3)$  servers and above. As such scalability to topologies of at least this scale is necessary. Furthermore, while a small test cluster may be feasibly reserved for experimentation [37], full-scale experimentation is not possible as this would require halting all or much of the services provided by the cluster (since the experimental allocation techniques would be unsuitable for service level requirements). Where a sufficiently accurate simulation of DCN patterns is not available - which it often isn’t [38–40] - and

a small cluster is reserved for experimentation, any algorithm developed on the small cluster must be consistent with respect to performance when transferred to the larger one.

All methods are evaluated on the basis of three metrics; acceptance ratio, CPU utilisation and memory utilisation. Acceptance ratio refers to the proportion of all requests received by some allocation method that were successfully allocated. CPU and memory utilisation refers to the proportion of the total amount of that resource that is available in the DC which is currently allocated to some request. We also observe utilisation metrics relating to each tier of the network, as well as the characteristic relationship between request size and how distributed it is throughout the DC for a particular method. These (baseline or agent). These observations are considered as emergent features (rather than performance-based metrics used to evaluate allocation policies), and are used to try to understand the nature of what each method (the proposed RL-based one in particular) does to achieve the allocation outcomes they do.

## B. Baselines

### Tetris

Tetris [25] is a multi-resource packing heuristic. It uses the cosine similarity between task requirement and server resource availability vectors to calculate scores upon which packing decisions are made. Network resources are considered to be those which are present at a particular server (e.g. how many free communication channels are available at a particular node), but does not account for less local network resources (e.g. resources across links  $n$ -hops away). It also imposes a score penalty on non-local resources in order to encourage locality in its decision making, whereby given an initially chosen server, the score of non-local (not in the same rack) will be slightly decreased. In this way an assumption about network resource efficiency is imposed which suggests that it is better to keep allocations rack local more than not.

### NALB

NALB is a network-aware resource allocation algorithm which uses a bandwidth-weighted breadth-first-search algorithm and a bandwidth-weighted  $k$ -shortest paths routing algorithm to find suitable nodes and establish connectivity between them respectively [5]. The algorithm accounts for CPU, memory, storage (not used in this work), bandwidth and/or latency, where relative weighting between bandwidth and latency is a tunable parameter of the algorithm. The resource environment in the work presented in this thesis is ‘heterogeneous’ with respect to each server (i.e. each server contains various resource types). As such the first server is chosen with a vectorised fitting procedure, similar to the Tetris method described above, instead of the original resource-contention based method designed for resource-homogeneous servers. Otherwise, all implementation features are identical to those presented in the paper introducing this method.

### NULB

NULB works similarly to the NALB method, except that the breadth-first-search algorithm does not use weighting. Weighting is still used for the  $k$ -shortest paths procedure [5].

### Random

Servers are selected randomly. Used as a lower bound on expected performance.

## 6. RESULTS

### A. DRL agent allocates more requests overall

On testing, the agent is observed to consistently outperform every baseline across each topology tested. For each topology, the percentage by which the agent improves over the best performing baseline on that topology is shown in Table 2. Most notably, it is seen that the agent thrives in particular when the network has few channels-per-links and/or when oversubscription is high (i.e. when the network is generally resource-constrained), achieving a 19.0%, 24.4% and 21.7% improvement for acceptance, CPU utilisation and memory utilisation respectively. Moreover, the agent is also able to find improvements even in the least resource-constrained environment where even the random baseline is comparable to some of the other baselines. It is also seen that, unsurprisingly, the agent achieves similarly improved resource utilisation for CPU and memory. In this case the same respective improvements are 5.8%, 2.7% and 2.7%. This is a natural emergent outcome of allocating more requests; higher acceptance ratio is equivalent to more requests occupying resources in the DC on average in a given moment in time. As such resource utilisation will also be higher on average.

### B. DRL agent is more consistent than baselines across different DCNs

The average performance at the end of the test episode for acceptance, CPU utilisation and memory utilisation are shown in Fig. 2. A key observation from these plots relating to both consistency and flexibility benefits is that while the RL method is always the best performing method on each topology, the baselines are frequently trading places for 2<sup>nd</sup>, 3<sup>rd</sup>, 4<sup>th</sup> and 5<sup>th</sup>.

As previously noted, heuristics are designed on the basis of some specific assumptions about a given system or problem, and are also tested in limited conditions. For example, the Tetris baseline assumes a statically defined emphasis on locality is beneficial, and also asserts that the network and node resources accounted for when scoring a particular server should be only its local ones (i.e. it's directly attached resources, as opposed to accounting for resources from nodes/links up to k-hops away, for example). This is not so say that heuristics are entirely inflexible; Tetris parameterises how much of a penalty non-local servers should receive, and NALB parameterises the weighting between latency and bandwidth in the routing process for when both features are used. However, the fundamental decision making processes as well as what information is used to make these decisions are for the most part static after the design and testing phase. In this sense a heuristic has some inherent bias in its behaviour that is derived from the design assumptions and test-performance feature-tuning, and as such do not necessarily have consistent performance benefits over some other heuristic in every circumstance. The tests whose results are shown in Table 2 and Fig. 2 differ only by the per-link resource quantity and share the fundamental topology. Even so, relatively simple variation is already enough to show the inconsistency of heuristics in this regard. Conversely, the agent learns appropriate policies for each network-resource profile and is able to consistently find better performance across each topology.

### C. DRL agent is more consistent than baselines with respect to request size

The plots shown in Fig. 8 (Appendix B) show the number of successful allocations of requests per method, where request sizes are grouped relative to the number of total servers worth

**Table 2.** Percentage improvement of the agent pair over the second best performing baseline for that topology across all tested topologies.

RL agent improvement over best baseline (%) (acceptance, CPU util., memory util.)				
Oversubscription				
		1:16	1:8	1:4
Chan.	8	19, 24, 22	15, 16, 20	22, 43, 23
per-link	16	9, 21, 16	11, 12, 15	8, 16, 11
tier-1	32	17, 17, 21	19, 12, 10	6, 3, 3

of resources that their specification rounds up to. This value is an integer between 1 and 8 inclusive. The reward structure is designed to be minimally imposing on the kind of policies the agent can learn, and as such is related only to how many requests it successfully allocates rather than some request-specific information (e.g. the resource requirement magnitude). This was done to attempt to influence the agent to learn policies that are 'fair' with respect to any request it encounters.

We expect from this design choice that the request should not learn to treat any particular size-range of request more carefully than others. To this end we analyse the number of accepted requests (per topology) aggregated over all test episodes and grouped by request size and explore whether the agent's advantage over the baselines is concentrated in certain kinds of requests, or distributed over all request sizes. We group requests by the minimum number of servers required to fulfill that resource request (1-8 inclusive). What is seen is that the agent's advantage is very consistent across not just topologies but also request size brackets. The only exceptions are for the 3 most resource-constrained topologies, where the agent incurs a small deficit in the largest request size brackets. The worst case is seen on the 8-channel 1:8 oversubscription ratio topology, where deficit of 10 and 2 requests for the requests in the 7-server and 8-server size brackets respectively. This amounts to 1.8% of the total number of requests received across this test, compared to an overall improvement of 15%, where all other request-size brackets are improved relative to the baselines.

### D. The agent requires less networking resources for the similar allocation performance

The agent's performance is also favourable compared against the baselines not just on the same topologies, but also across topologies. In particular, the agent can enable higher acceptance ratio on lower-resource topologies than the best performing baseline on higher-resource topologies. In the most extreme case observed across all experiments, the agent achieves an acceptance on the 8-channel 1:16 oversubscription topology that is only 1% lower than what the best performing baseline achieves on the 32-channel 1:16 oversubscription topology. In this case, the agent is effectively allowing for the same resource allocation service level to be achieved with 3× less resources.

Practically speaking, this is a very desirable feature. While optical DCN networks can allow various scalability issues to be avoided, the disaggregated resource paradigm that they enable imposes heavy demand on the network. An allocation policy



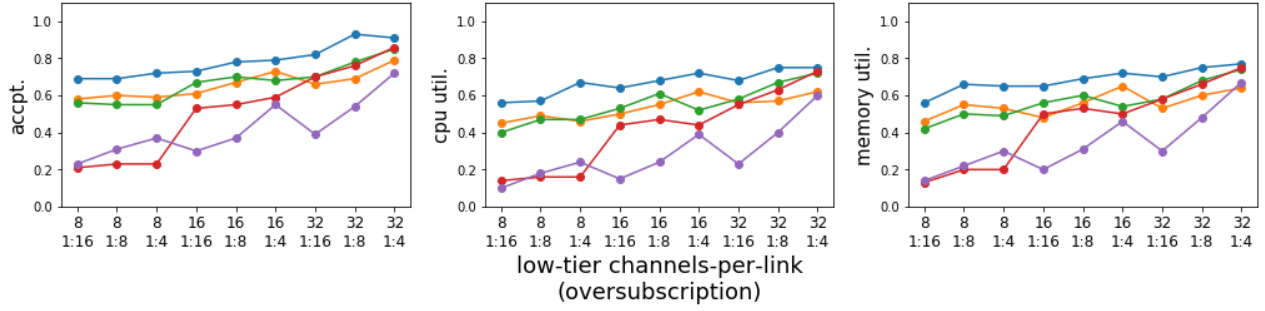


**Fig. 2.** blue=RL agent, orange=Tetris, green=NALB, red=NULB, purple=random. Line plots showing the acceptance ratio (top), CPU utilisation (middle) and memory utilisation (bottom) for each method when tested on each topology. Topology labels (x-axis) are defined as  $\frac{\text{channels per tier} - 1 \text{ links}}{\text{oversubscription}}$

**Table 3**

RL agent performance delta on larger topologies (%)  
(acceptance, CPU util., memory util.)

		Oversubscription		
		1:16	1:8	1:4
Low-tier	8.0	6, 4, 0	6, -12, -2	4, 13, 6
channels	16.0	16, 8, 14	10, 3, 10	9, 4, 11
per-link	32.0	7, 4, 11	-6, 8, 3	-1, -1, 6

that is able to minimise the amount of networking resources required to maintain some level of resource efficiency can allow for such systems to be built more feasibly. Large network infrastructure requirements (e.g. lots of fibre and switches) is expensive and requires much maintenance and planning [41]. Minimising these requirements is highly desirable to limit initial capital, operational and maintenance costs of such systems.

### E. Topology scale-up performance

Table 3 shows the percentage delta in test performance for the DRL agent when applied to each topology vs its  $\mathcal{O}(10^2)$  scaled up version. In the table +ve indicates that the large-topology score was better and -ve indicates that it was worse. Averaged across each topology, the delta is 5.6%, 3.4% and 6.5% for acceptance, CPU utilisation and memory utilisation respectively. The key indication from these results is simply that the agent is clearly able to learn a policy on a small graph that accounts for features of the topology and request distribution that are valid when applied to much larger topologies and over a much longer series of requests.

### F. Interpreting the policy's allocation strategy

Here is presented a discussion, led by visual analysis, on the nature of the allocation policy that is learnt by the DRL agent. Since it is unclear how to directly extract policy principles from neural networks directly, numerical and visual analysis through experimental probing is required to infer as best as possible what the policy is doing. In effect, this section attempts to describe the learnt allocation policy as if it were a heuristic.

#### F.1. DRL agent uses network when it is available

Figure 3 shows the utilisation of each tier's network resources per-topology-per-method. Looking at the agent's results, it is seen that when the network resources are very limited (highly oversubscribed and few channels-per-link), the method concentrates allocations within racks, having higher utilisation for tier-1 (intra-rack) and comparatively very low utilisation for the higher tiers. As the agent moves towards topologies with lower oversubscription / more channels-per-link, the tier-2 and tier-3 resources are more highly utilised and the tier-1 resources less. This indicates that the agent learns a policy that exploits network resources when they are available, but allocates more rack-locally when they are not. Moreover, the biggest increase in utilisation occurs at tier-3, which increases from  $\approx 0.2$  to  $\approx 0.8$  between the most and least network-resource constrained topologies. This indicates that in particular the agent learns to exploit the most non-local allocation possible (inter-cluster) when network resources are available to do so.

Similarly, Figure 5 provides a more aggregated but intuitive representation of how the policy exploits the network in various oversubscription scenarios. Each distribution shows the combined results of allocation outcomes for all topologies of a particular oversubscription ratio (per-method). The x-axis refers to how distributed the servers allocated to a request were, and the y-axis indicates how commonly that distribution was used by an allocation method. Distribution outcomes (intra-server, intra-rack, intra-cluster and inter-cluster) are presented continuously rather than discretely, since mixtures are generally possible (i.e. it might be the case that 90% of the servers allocated to a request are in the same rack and the other 10% are in a neighbouring rack meaning that the request is mostly intra-rack and partially intra-cluster). Observing how the distributions change moving from oversubscription of 1:16 through to 1:8 and 1:4, a similar conclusion as described above can be drawn. In the 1:16 oversubscribed topology, the agent is almost entirely intra-rack. As the network opens up more in the 1:8 oversubscription case it can be seen that more requests are distributed intra-cluster (across neighbouring racks) but inter-cluster allocations are insignificant. Finally in the most network-resourced topology with 1:4 oversubscription, the agent reduces its dependency on intra-rack allocations significantly, allocating nearly as many intra-cluster and inter-cluster as it does intra-rack (though intra-rack still remains the dominant allocation outcome due to racks having the most network resources per connected server. By comparison, the distributions for each heuristic are notably much more static when self-compared across oversubscription ratios, since it is the

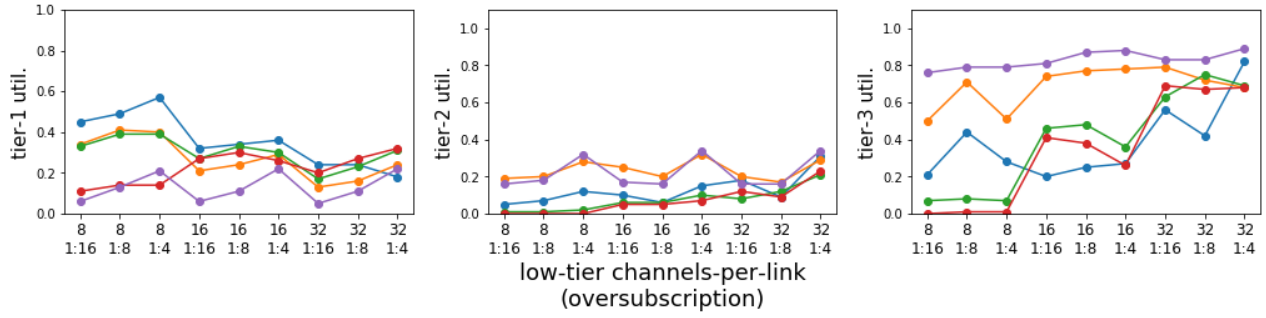


**Fig. 3.** blue=RL agent, orange=Tetris, green=NALB, red=NULB, purple=random. Line plots showing the utilisation of tier-1 (top), tier-2 (middle) and tier-3 (bottom) networking resources for each method when tested on each topology. Topology labels (x-axis) are defined as  $\frac{\text{channels per tier-1 link}}{\text{oversubscription}}$

exact same policy deployed in each case. While Tetris changes slightly between 1:8 and 1:4 oversubscription to exploit intra-cluster with a slightly high proportion, the NALB and NULB maintain almost exactly the same shape indicating that their network-usage is independent of what is actually available.

## F.2. The agent distributes requests differently based on their resource requirements

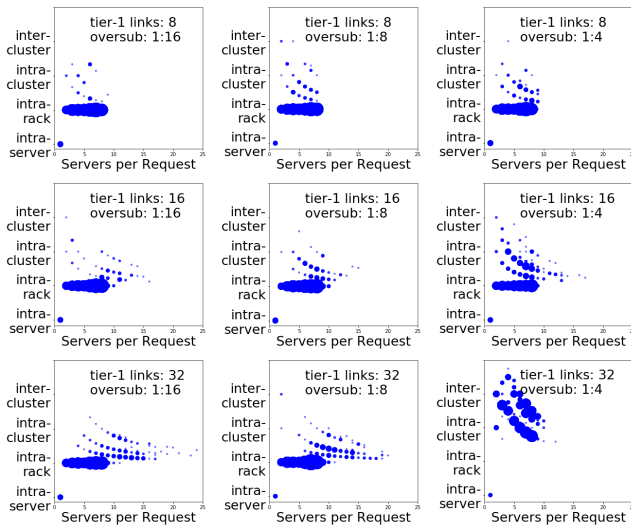


**Fig. 4.** Visualising the deep reinforcement learning agent's policy with respect to relationship between how many servers were allocated to a request, and how distributed those servers were for that request. Blue dots represent server-distribution pairs and their size represents how many requests were served at this combination. Shown for each training topology.

Following the conclusions discussed in section F.1, further questions can be asked about how the agent learns to exploit network resource availability in relation to the specific request. Specifically, what relationship does the agent learn between request size and how distributed that request should be to maximise the possibility of finding acceptable allocations over the long term?

Figure 4 shows (for each oversubscription/channels-per-link topology combination) a relationship between how many servers were allocated to a request (x axis) and how distributed those servers were (y axis). In the figures, the size of a blue

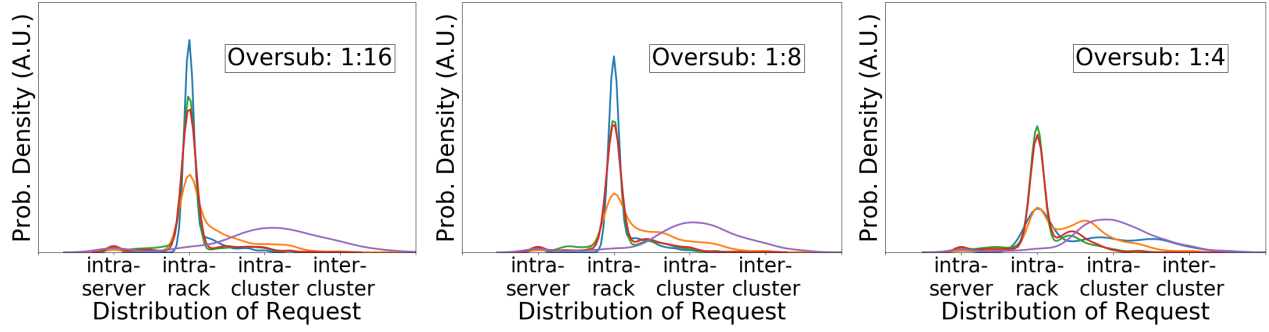
circle relates to the number of requests which were allocated that number of servers and distributed at that amount. Figure 6 shows a 2D colour-scaled plot where the x and y axes refer to the number of CPU and memory units requested and the colour of a point indicates how distributed the request with those requirements was distributed. These two plots allow us to consider a relationship between request size, how many servers across which that request was allocated and how those servers were distributed. Note that down-column comparison looks at increasing the channels-per-link quantity, and comparing sub-figures down-row compares decreasing the oversubscription ratio (less oversubscription).

Figure 4 shows that while there is a preference for intra-rack allocation for on all topologies, a slightly increased preference for greater distribution is seen as the amount of networking resources increases. The most highly distributed requests are also generally the smaller ones using few servers rather than the larger requests with many servers. Fig 6 shows a trend of generally increasing distribution as network resources increase. This trend is more common among the smaller requests who's likelihood of being more distributed increases most notably with increasing network resources. On the contrary, the largest requests tend to remain predominantly rack-local, even as total networking resources increase. Finally, there is also a general preference for rack-locality since the overall majority of requests (observed over all size brackets) are rack local.

This behaviour can be summarised as 1. rack-local allocations are generally preferred; 2. smaller requests have a higher likelihood of being more highly distributed; 3. larger requests have a higher likelihood of being less distributed and kept rack-local.

Higher tiers of the network are accessible by any server in the DCN. The higher the tier, the more servers are likely to use it's resources. Conversely, lower tiers of the network are likely to be accessed by their directly attached servers, or a server who wishes to communicate with that server. Larger requests require more servers, and therefore more network resources to interconnect them, whereas smaller requests require fewer network resources correspondingly. What is evident from the policy visualisation and analysis is that the agent learns to tactically use network resources in a way that prevents large requests from congesting the the higher tiers of the network for other requests that arrive in the future. Smaller requests are allocated in a way such that lower-oversubscription (less contended for) regions of the network are kept free for the more demanding larger requests, and smaller requests tend to be more distributed without using





**Fig. 5.** blue=RL agent, orange=Tetris, green=NALB, red=NULB, purple=random. Line plots showing the acceptance ratio (top), CPU utilisation (middle) and memory utilisation (bottom) for each method when tested on each topology. Topology labels (x-axis) are defined as  $\frac{\text{channels per tier-1 links}}{\text{oversubscription}}$

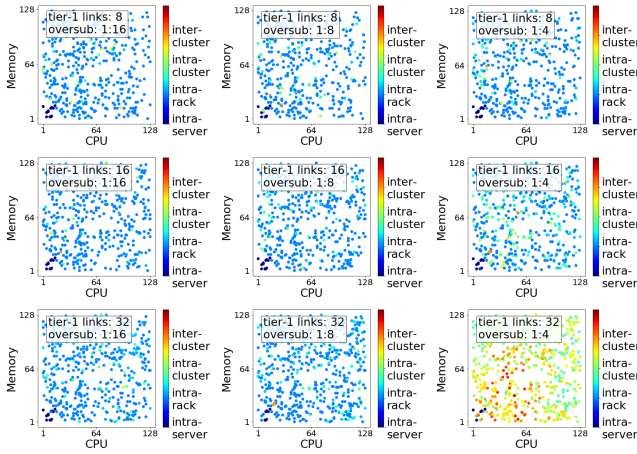


**Fig. 6.** Visualising the deep reinforcement learning agent's policy with respect to the relationship between requested CPU units, requested memory units and how distributed the allocated request at that size was. Distribution is represented by colour, where blue to red corresponds to more less to more distributed. Shown for each training topology.

excessive higher tier network resources and prohibiting future allocations.

## 7. CONCLUSION

This paper shows that deep reinforcement learning with graph neural network based policy architectures can be used to learn effective network-aware resource allocation policies end-to-end. When trained and tested across 9 data centre topologies with different network-resource quantity and oversubscription, the presented method achieves up to a 19%, 24% and 22% improvement for acceptance ratio, CPU utilisation and memory utilisation respectively against a number of baseline heuristics for network-aware resource allocation. Improvements are most pronounced when the network resources are most limited. The method also achieves the same performance as the best heuristic whilst requiring  $3\times$  less network resources to do so. Additionally, the policy is highly scalable and the policy architecture topology agnostic. When trained on topologies with  $\mathcal{O}(10^1)$  servers, policy performance is highly consistent when deployed on topologies with the same oversubscription properties but  $\mathcal{O}(10^3)$  more servers with no re-training or architectural adjust-

ments required.

Avenues of future work include training a single agent for a multiple of topologies/network-types; increasing the scale of test topologies beyond the  $\mathcal{O}(10^3)$  shown here; handling a wider variety of request types (e.g. different requests requiring different connectivity patterns to all-to-all); greater variety/time-dependent request distributions to be handled during allocation rather than a single static one and more restrictive requests where latency requirements are stated explicitly, not implicitly satisfied by the network and must be accounted for in allocation strategies.

## ACKNOWLEDGEMENTS

This work was supported under the Engineering and Physical Sciences Research Council (EP/R041792/1 and EP/L015455/1), the Industrial Cooperative Awards in Science and Technology (EP/R513143/1), the OptoCloud (EP/T026081/1), and the TRANSNET (EP/R035342/1) grants.

## DISCLOSURES

The authors do not maintain any conflicts of interest related to this project.

## REFERENCES

1. O. Hadary, L. Marshall, I. Menache, A. Pan, E. E. Greeff, D. Dion, S. Dorminey, S. Joshi, Y. Chen, M. Russinovich, and T. Moscibroda, "Protean: VM allocation service at scale," in *14th USENIX Symposium on Operating Systems Design and Implementation (OSDI 20)*, (USENIX Association, 2020), pp. 845–861.
2. D. A. Popescu, "Latency-driven performance in data centres," Ph.D. thesis (2019).
3. polatis.com, "Series 7000 - 384x384 port software-defined optical circuit switch,".
4. G. Zervas, F. Jiang, Q. Chen, V. Mishra, H. Yuan, K. Katrinis, D. Syrivelis, A. Reale, D. Pnevmatikatos, M. Enrico, and N. Parsons, "Disaggregated compute, memory and network systems: A new era for optical data centre architectures," in *Optical Fiber Communication Conference*, (Optical Society of America, 2017), p. W3D.4.
5. G. Zervas, H. Yuan, A. Saljoghei, Q. Chen, and V. Mishra, "Optically disaggregated data centers with minimal remote memory latency: Technologies, architectures, and resource allocation," *J. Opt. Commun. Netw.* **10**, A270–A285 (2018).
6. V. Mishra, J. L. Benjamin, and G. Zervas, "Monet: heterogeneous memory over optical network for large-scale data center resource disaggregation," *IEEE/OSA J. Opt. Commun. Netw.* **13**, 126–139 (2021).

7. F. E. Blog, *Efficient, reliable cluster management at scale with Tupperware* (2019).
8. M. Isard, V. Prabhakaran, J. Currey, U. Wieder, K. Talwar, and A. Goldberg, "Quincy: Fair scheduling for distributed computing clusters," in *Proceedings of the ACM SIGOPS 22nd Symposium on Operating Systems Principles*, (Association for Computing Machinery, New York, NY, USA, 2009), SOSP '09, p. 261–276.
9. A. Verma, L. Pedrosa, M. R. Korupolu, D. Oppenheimer, E. Tune, and J. Wilkes, "Large-scale cluster management at google with borg," in *Proceedings of the European Conference on Computer Systems (EuroSys)*, (Bordeaux, France, 2015).
10. M. Schwarzkopf, A. Konwinski, M. Abd-El-Malek, and J. Wilkes, "Omega: flexible, scalable schedulers for large compute clusters," in *SIGOPS European Conference on Computer Systems (EuroSys)*, (Prague, Czech Republic, 2013), pp. 351–364.
11. O. Vinyals, M. Fortunato, and N. Jaitley, "Pointer networks," (2015).
12. I. Bello, H. Pham, Q. V. Le, M. Norouzi, and S. Bengio, "Neural combinatorial optimization with reinforcement learning," CoRR. **abs/1611.09940** (2016).
13. H. Mao, M. Alizadeh, I. Menache, and S. Kandula, "Resource management with deep reinforcement learning," in *Proceedings of the 15th ACM Workshop on Hot Topics in Networks*, (Association for Computing Machinery, New York, NY, USA, 2016), HotNets '16, p. 50–56.
14. E. Khalil, H. Dai, Y. Zhang, B. Dilkina, and L. Song, "Learning combinatorial optimization algorithms over graphs," in *Advances in Neural Information Processing Systems 30*, I. Guyon, U. V. Luxburg, S. Bengio, H. Wallach, R. Fergus, S. Vishwanathan, and R. Garnett, eds. (Curran Associates, Inc., 2017), pp. 6348–6358.
15. R. Ying, R. He, K. Chen, P. Eksombatchai, W. L. Hamilton, and J. Leskovec, "Graph convolutional neural networks for web-scale recommender systems," CoRR. **abs/1806.01973** (2018).
16. A. Mittal, A. Dhawan, S. Medya, S. Ranu, and A. Singh, "Learning heuristics over large graphs via deep reinforcement learning," (2019).
17. Z. Li, Q. Chen, and V. Koltun, "Combinatorial optimization with graph convolutional networks and guided tree search," in *Advances in Neural Information Processing Systems 31*, S. Bengio, H. Wallach, H. Larochelle, K. Grauman, N. Cesa-Bianchi, and R. Garnett, eds. (Curran Associates, Inc., 2018), pp. 539–548.
18. T. D. Barrett, W. R. Clements, J. N. Foerster, and A. I. Lvovsky, "Exploratory combinatorial optimization with reinforcement learning," CoRR. **abs/1909.04063** (2019).
19. R. Addanki, S. B. Venkatakrishnan, S. Gupta, H. Mao, and M. Alizadeh, "Placeto: Learning generalizable device placement algorithms for distributed machine learning," arXiv preprint arXiv:1906.08879 (2019).
20. H. Mao, M. Schwarzkopf, S. B. Venkatakrishnan, Z. Meng, and M. Alizadeh, "Learning scheduling algorithms for data processing clusters," in *Proceedings of the ACM Special Interest Group on Data Communication*, (Association for Computing Machinery, New York, NY, USA, 2019), SIGCOMM '19, p. 270–288.
21. P. Almasan, J. Suarez-Varela, A. Badia-Sampera, K. Rusek, P. Barlet-Ros, and A. Cabello, "Deep reinforcement learning meets graph neural networks: An optical network routing use case," (2019).
22. H. Yao, X. Chen, M. Li, P. Zhang, and L. Wang, "A novel reinforcement learning algorithm for virtual network embedding," *Neurocomputing* **284**, 1 – 9 (2018).
23. Z. Yan, J. Ge, Y. Wu, L. Li, and T. Li, "Automatic virtual network embedding: A deep reinforcement learning approach with graph convolutional networks," *IEEE J. on Sel. Areas Commun.* **38**, 1040–1057 (2020).
24. H. Yuan, A. Saljoghei, A. Peters, and G. Zervas, "Disaggregated optical data center in a box network using parallel ocs topologies," in *Optical Fiber Communication Conference*, (Optical Society of America, 2018), p. W1C.2.
25. R. Grandl, G. Ananthanarayanan, S. Kandula, S. Rao, and A. Akella, "Multi-resource packing for cluster schedulers," in *Proceedings of the 2014 ACM Conference on SIGCOMM*, (Association for Computing Machinery, New York, NY, USA, 2014), SIGCOMM '14, p. 455–466.
26. Z. Shabka and G. Zervas, "Nara: Learning network-aware resource allocation algorithms for cloud data centres," CoRR. **abs/2106.02412** (2021).
27. R. S. Sutton and A. G. Barto, *Reinforcement Learning: An Introduction* (A Bradford Book, Cambridge, MA, USA, 2018).
28. D. Silver, T. Hubert, J. Schrittwieser, I. Antonoglou, M. Lai, A. Guez, M. Lanctot, L. Sifre, D. Kumaran, T. Graepel, T. P. Lillicrap, K. Simonyan, and D. Hassabis, "Mastering chess and shogi by self-play with a general reinforcement learning algorithm," CoRR. **abs/1712.01815** (2017).
29. O. Vinyals, I. Babuschkin, W. M. Czarnecki, M. Mathieu, A. Dudzik, J. Chung, D. H. Choi, R. Powell, T. Ewalds, P. Georgiev, J. Oh, D. Horgan, M. Kroiss, I. Danihelka, A. Huang, L. Sifre, T. Cai, J. P. Agapiou, M. Jaderberg, A. S. Vezhnevets, R. Leblond, T. Pohlen, V. Dalibard, D. Budden, Y. Sulsky, J. Molloy, T. L. Paine, C. Gulcehre, Z. Wang, T. Pfaff, Y. Wu, R. Ring, D. Yogatama, D. Wünsch, K. McKinney, O. Smith, T. Schaul, T. Lillicrap, K. Kavukcuoglu, D. Hassabis, C. Apps, and D. Silver, "Grandmaster level in StarCraft II using multi-agent reinforcement learning," *Nature*. **575**, 350–354 (2019).
30. P. Veličković, G. Cucurull, A. Casanova, A. Romero, P. Liò, and Y. Bengio, "Graph attention networks," in *International Conference on Learning Representations*, (2018).
31. W. Hamilton, Z. Ying, and J. Leskovec, "Inductive representation learning on large graphs," in *Advances in Neural Information Processing Systems*, vol. 30 I. Guyon, U. V. Luxburg, S. Bengio, H. Wallach, R. Fergus, S. Vishwanathan, and R. Garnett, eds. (Curran Associates, Inc., 2017).
32. T. N. Kipf and M. Welling, "Semi-supervised classification with graph convolutional networks," in *5th International Conference on Learning Representations, ICLR 2017, Toulon, France, April 24-26, 2017, Conference Track Proceedings*, (OpenReview.net, 2017).
33. E. Liang, R. Liaw, R. Nishihara, P. Moritz, R. Fox, J. Gonzalez, K. Goldberg, and I. Stoica, "Ray rllib: A composable and scalable reinforcement learning library," CoRR. **abs/1712.09381** (2017).
34. M. Wang, D. Zheng, Z. Ye, Q. Gan, M. Li, X. Song, J. Zhou, C. Ma, L. Yu, Y. Gai, T. Xiao, T. He, G. Karypis, J. Li, and Z. Zhang, "Deep graph library: A graph-centric, highly-performant package for graph neural networks," arXiv preprint arXiv:1909.01315 (2019).
35. T. Pohlen, B. Piot, T. Hester, M. G. Azar, D. Horgan, D. Budden, G. Barth-Maron, H. van Hasselt, J. Quan, M. Večerík, M. Hessel, R. Munos, and O. Pietquin, "Observe and look further: Achieving consistent performance on atari," (2018).
36. C. W. F. Parsonson, A. Laterre, and T. D. Barrett, "Reinforcement learning for branch-and-bound optimisation using retrospective trajectories," (2022).
37. A. Roy, H. Zeng, J. Bagga, G. Porter, and A. C. Snoeren, "Inside the social network's (datacenter) network," *SIGCOMM Comput. Commun. Rev.* **45**, 123–137 (2015).
38. C. W. Parsonson, J. L. Benjamin, and G. Zervas, "Traffic generation for benchmarking data centre networks," *Opt. Switch. Netw.* **46**, 100695 (2022).
39. B. Sharma, V. Chudnovsky, J. L. Hellerstein, R. Rifaat, and C. R. Das, "Modeling and synthesizing task placement constraints in google compute clusters," in *Proceedings of the 2nd ACM Symposium on Cloud Computing*, (2011), pp. 1–14.
40. E. Cortez, A. Bonde, A. Muzio, M. Russinovich, M. Fontoura, and R. Bianchini, "Resource central: Understanding and predicting workloads for improved resource management in large cloud platforms," in *Proceedings of the 26th Symposium on Operating Systems Principles*, (Association for Computing Machinery, New York, NY, USA, 2017), SOSP '17, p. 153–167.
41. L. Poutievski *et al.*, "Jupiter evolving: Transforming google's datacenter network via optical circuit switches and software-defined networking," in *Proceedings of the ACM SIGCOMM 2022 Conference*, (Association for Computing Machinery, New York, NY, USA, 2022), SIGCOMM '22, p. 66–85.

## A. VISUALISATION OF THE TRAINING TOPOLOGY

Fig. 7 shows a simple visualisation of the 3-tier DCN topology used for training. Racks consist of groups of 16 servers, and

clusters consist of groups of 2 racks. There are 2 clusters total in this training topology.

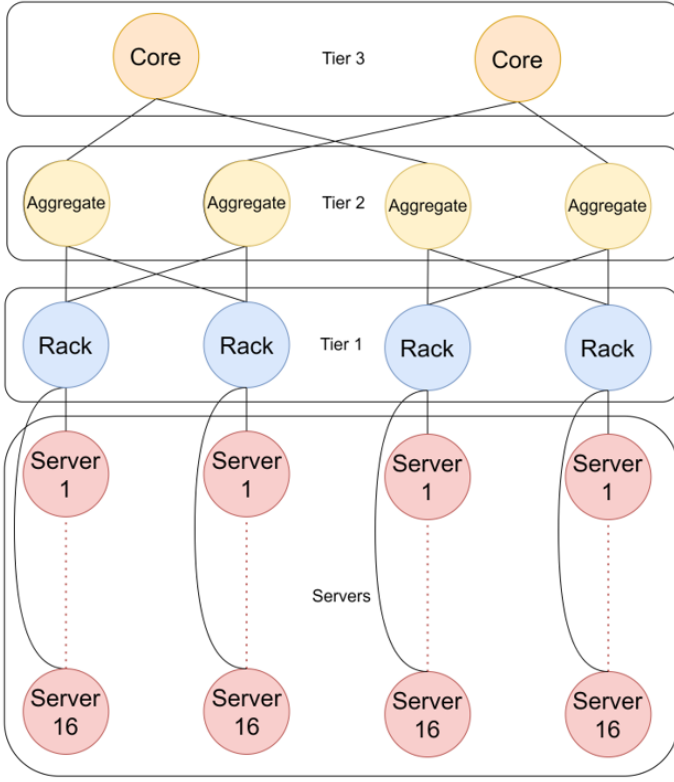


**Fig. 7.** Simple illustration of the data centre network used for training and testing in this work, where the rack-grouping of servers and tier'd structure of the network is labelled explicitly.

## B. BAR PLOTS FOR ACCEPTED REQUESTS

The plots in Fig. 8 show the topology-specific results for allocation success with respect to allocation size (relative to the minimum number of servers required to allocate that request).

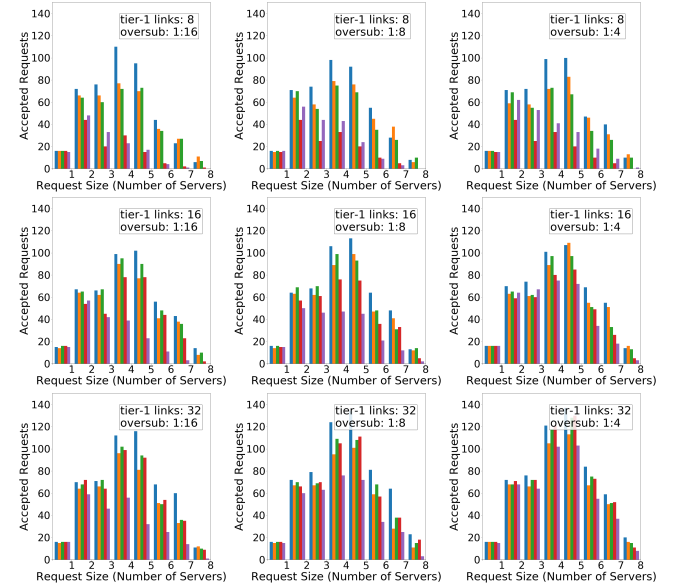


**Fig. 8.** blue=RL agent, orange=Tetris, green=NALB, red=NULB, purple=random.

Histograms showing how many requests were successfully allocated by each method, grouped by how many servers worth of total resources were requested (i.e. what is the minimum number of servers that could theoretically fulfil this request). Text on the sub-figures refers to which topology the results are for with respect to its networking resources and oversubscription (as in the rest of the paper).